51st IEEE Conference on Decision and Control
December 10-13, 2012. Maui, Hawaii, USA

Aircraft Control based on Fast Non-linear MPC & Multiple-shooting

Sébastien Gros, Rien Quirynen and Moritz Diehl

Abstract— **For extreme maneuvers, feasible flight trajectories can be difficult to compute. If the aircraft is controlled based on linear approximations of the system dynamics that are computed along infeasible trajectories, poor control actions and violations of the flight envelope constraints can result. This paper proposes a Non-linear Model Predictive Control (NMPC) approach, to handle extreme maneuvers, respect the flight envelope, handle actuator failure, and perform emergency obstacle avoidance with a single, non-hierarchical controller that can be implemented in real time.**

Keywords **: aircraft control, extreme manoeuvre, fault-tolerant control, obstacle avoidance, fast NMPC, multiple-shooting.**

I. INTRODUCTION

The performance requirements for modern aircraft lead to designs having larger aspect ratios and a lower structural weight, yielding tighter flight envelope, and more involved flight characteristics. Extreme or emergency maneuvers with high-performance aircraft are likely to be performed at the limits of the flight envelope and actuator capabilities, hence requiring flight controllers that can take the aircraft limitations explicitly into account while fully exploiting its dynamics. As one example, in the context of Airborne Wind Energy (AWE) [11], light, high-performance wings have to repeatedly perform aerobatic maneuvers, and actuator failure or tether rupture are bound to happen in extreme configurations. In this context, fault-tolerant control that can recover the aircraft from an extreme configuration is a key component to the safety and performance of the system.

As a second example, the growing demand for Unmanned Aerial Vehicles (UAVs) has motivated the improvement of controllers for autonomous flight. More specifically, because UAVs will be required to operate at a high level of safety and in complex environments, fault-tolerant control and obstacle avoidance have become important research topics. Aircraft limitations and actuator failures are straightforward to handle in the framework of Model Predictive Control (MPC), which has therefore been recognized as an ideal framework to develop modern, fault-tolerant flight controllers [9], [10], [12], [13].

Linear MPC is typically based on a linear time-varying approximation of the aircraft dynamics and constraints, calculated along a pre-defined reference trajectory. For aggressive maneuvers, or in the case of obstacle avoidance, computing feasible reference trajectories is often an involved task. Due to perturbations, changes of flight mission, or unexpected obstacles, reference trajectories needs to be regularly recomputed online.

In this context, the computation of new reference trajectories and the system re-linearization is ideally performed as often as possible based on the latest information on the aircraft state, status, and required flight mission. The problem is therefore best cast as a Non-Linear Model Predictive Control (NMPC) problem, which re-linearizes the system along its current predicted trajectory rather than along the reference trajectory. NMPC schemes are, however, often deemed too slow to tackle the control of fast systems. This paper proposes an NMPC formulation that can be implemented in real-time, and treat the problem of tracking infeasible, extreme reference trajectories, respect the aircraft flight envelope, manage actuator faults and perform obstacle avoidance within a single, non-hierarchical controller.

The paper is organized as follows. Section II proposes a simple aircraft model capturing the major effects encountered in a high-performance aircraft. Section III proposes a single NMPC formulation that tackles the different aspects of flight control. Section IV describes the solution approach to solve the proposed NMPC problem in real-time. Section V shows simulation results to illustrate the proposed approach.

Contribution: a fault-tolerant control scheme based on fast NMPC, sufficiently fast for a real-time implementation, capable of handling extreme maneuvers, a tight flight envelope, actuator faults and emergency obstacle avoidance.

II. AIRCRAFT MODEL

This section presents the aircraft model proposed for efficient NMPC. For the sake of clarity, the model is kept simple, considering only the major effects contributing to the aircraft behavior. However, increasing the model complexity is not a major problem in the proposed control framework.

A. Dynamics

The aircraft time evolution is described by the motion of a single 6-DOF rigid body. The body position and velocity in the inertial reference frame E are given by $p \in \mathbb{R}^3$ and $v \in \mathbb{R}^3$ respectively. The aircraft attitude is defined by the rotation matrix R operating the change of coordinates from the aircraft reference frame e back to the inertial reference frame E. The time evolution of the aircraft attitude is defined by the angular velocity vector ω describing the angular velocity of frame e with respect to frame E, given in e (see Fig. 1). The time evolution of p, v, R, ω is given by:

$$\begin{aligned} \dot{p} &= v, \quad m\dot{v} = F(p,v,R,\omega) - g\mathbf{1}_z, \\ \dot{R} &= R\Omega, \quad I\dot{\omega} = T(p,v,R,\omega) + \omega \times I\omega \end{aligned} \tag{1}$$

S. Gros, R. Quirynen and M. Diehl are with the Optimization in Engineering Center (OPTEC), K.U. Leuven, Kasteelpark Arenberg 10, B-3001 Leuven-Heverlee, Belgium. sgros@esat.kuleuven.be

978-1-4673-2066-5/12/$31.00 ©2012 IEEE

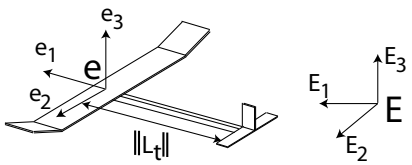


Fig. 1. System schematic

where $\mathbf{1}_z = \begin{bmatrix} 0 & 0 & 1 \end{bmatrix}$, g is the gravity, $\Omega \in so(3)$ is the skew-matrix generated by the angular velocity vector ω, i.e.

$$\Omega = \begin{bmatrix} 0 & -\omega_3 & \omega_2 \\ \omega_3 & 0 & -\omega_1 \\ -\omega_2 & \omega_1 & 0 \end{bmatrix},$$

and T and F are the aerodynamic moments and forces respectively. In the following, the vectors $e_{1,2,3} \in \mathbb{R}^3$ will denote the columns of matrix R, i.e.:

$$R = \begin{bmatrix} e_1 & e_2 & e_3 \end{bmatrix}.$$

The body reference frame is chosen such that e_1, e_2 and e_3 span the aircraft longitudinal, transversal and vertical axis respectively (see Fig. 1).

The aircraft state vector X is given by $X^T = \begin{bmatrix} p^T & v^T & e_1^T & e_2^T & e_3^T & \omega \end{bmatrix}$.

B. Forces and moments

The aircraft relative velocity vector in the body reference frame E, $V^{\mathrm{E}} \in \mathbb{R}^3$ is given by:

$$V^{\mathrm{E}} = R^T V, \quad V = v - w,$$

where $w \in \mathbb{R}^3$ is the local wind velocity vector. The tail relative velocity vector in the body reference frame E, $V^t \in \mathbb{R}^3$, including the relative velocity induced by the angular velocity ω is given by:

$$V^{\mathrm{t}} = V^{\mathrm{E}} - \omega \times L_{\mathrm{t}}$$

where $L_t \in \mathbb{R}^3$ is the position of the tail in the body reference frame E. The aircraft angle of attack (AoA) α, side-slip angle β, tail angle of attack α^{t} and tail side-slip angle β^{t}, are approximated by:

$$\begin{aligned} \alpha &= -\frac{V_3^{\mathrm{E}}}{V_1^{\mathrm{E}}}, \quad \alpha^{\mathrm{t}} = \alpha_0^{\mathrm{t}} - \frac{V_3^{\mathrm{t}}}{V_1^{\mathrm{t}}}, \\ \beta &= \frac{V_2^{\mathrm{E}}}{\sqrt{\left(V_1^{\mathrm{E}}\right)^2 + \left(V_3^{\mathrm{E}}\right)^2}}, \quad \beta^{\mathrm{t}} = \frac{V_2^{\mathrm{t}}}{\sqrt{\left(V_1^{\mathrm{t}}\right)^2 + \left(V_3^{\mathrm{t}}\right)^2}}. \end{aligned}$$

where $V_{1,2,3}^{\mathrm{E}} \in \mathbb{R}$ and $V_{1,2,3}^{\mathrm{t}} \in \mathbb{R}$ are the components of the relative velocity vectors of the aircraft and of the tail respectively, and α_0 is the stabilizer trim angle.

The lift force is assumed to be orthogonal to the relative velocity and to the wing transversal axis, hence it is spanned by the vector:

$$e^{\mathrm{L}} = e_2 \times V^{\mathrm{E}},$$

normed to V. The lift and drag coefficients and the resulting aerodynamic forces are then given by:

$$\begin{aligned} C_{\mathrm{L}} &= C_{\mathrm{L}}^{\alpha}\alpha, \\ C_{\mathrm{D}} &= C_{\mathrm{D}}^{0} + C_{\mathrm{D}}^{\alpha}\alpha^2 + C_{\mathrm{D}}^{\beta}\beta^2 \\ F_{\mathrm{L}} &= \frac{1}{2}\rho A C_{\mathrm{L}} e^{\mathrm{L}} \|V\|, \quad F_D = -\frac{1}{2}\rho A C_{\mathrm{D}} V \|V\|. \end{aligned}$$

The roll, pitch and yaw coefficients and the resulting aerodynamic moments are given by:

$$\begin{aligned} C_{\mathrm{R}} &= C_{\mathrm{R}}^{\mathrm{u}} u_1 + C_{\mathrm{R}}^{\mathrm{l}} \omega_{\mathrm{l}} + C_{\mathrm{R}}^{3} \omega_3, \\ C_{\mathrm{P}} &= C_{\mathrm{P}}^{\mathrm{u}} u_2 + C_{\mathrm{P}}^{\mathrm{T}} \alpha^{\mathrm{t}} + C_{\mathrm{P}}^{\alpha} \alpha, \\ C_{\mathrm{Y}} &= C_{\mathrm{Y}}^{\mathrm{u}} u_3 + C_{\mathrm{Y}}^{\mathrm{l}} \omega_{\mathrm{l}} + C_{\mathrm{Y}}^{\mathrm{T}} \beta^{\mathrm{t}}, \\ T_{\mathrm{R,P,Y}} &= \frac{1}{2}\rho A C_{\mathrm{R,P,Y}} \|V\|^2, \end{aligned}$$

where u_1, u_2 and u_3 are the ailerons, elevator and rudder deflexion respectively, with maximum deflexion normed to 1. Coefficients C_{R}^3 and $C_{\mathrm{Y}}^{\mathrm{l}}$ model the adverse yaw and roll respectively. Coefficient $C_{\mathrm{R}}^{\mathrm{l}}$ models the roll damping. Coefficients $C_{\mathrm{P}}^{\mathrm{t}}$ and $C_{\mathrm{Y}}^{\mathrm{t}}$ model the pitch and yaw moment introduced by the tail angles and motion.

C. Actuators

The engine thrust is assumed to be aligned with the aircraft longitudinal axis e_1. The force yielded by the engine is given by $F_{\mathrm{Thrust}} = e_1 T_{\max} u_4$, where $u_4 \in [0,1]$ is the fraction of the maximum engine thrust $T_{\max} \in \mathbb{R}$. For sake of simplicity, it is assumed here that the engine can be modeled by a first-order dynamics, bounded amplitude and rate of change, i.e.:

$$\dot{u}_4 = \frac{1}{\tau_{\mathrm{h}}}\left(u_4^{\mathrm{ref}} - u_4\right), \quad |\dot{u}_4| \le \dot{u}_4^{\max}, \quad 0 \le u_4 \le 1.$$

It is assumed here that the engine can only yield a positive thrust. The control surface dynamics are modeled by bounded rates of change, and bounded amplitude i.e.

$$|u_i| \le u_i^{\max}, \quad |\dot{u}_i| \le \dot{u}_i^{\max}, \quad i = 1,2,3.$$

Summing up all the forces and moments contributing to the aircraft behavior, F and T in (1) are given by:

$$\begin{aligned} F &= F_{\mathrm{L}} + F_{\mathrm{D}} + F_{\mathrm{Thrust}}, \\ T &= \begin{bmatrix} T_{\mathrm{R}} & T_{\mathrm{P}} & T_{\mathrm{Y}} \end{bmatrix}^T. \end{aligned}$$

The state, and control of the controlled system vectors are chosen as

$$\begin{aligned} X^T &= \begin{bmatrix} p^T & v^T & e_1^T & e_2^T & e_3^T & \omega^T & u_1 & u_2 & u_3 & u_4 \end{bmatrix}, \\ U &= \begin{bmatrix} \dot{u}_1 & \dot{u}_2 & \dot{u}_3 & u_4^{\mathrm{ref}} \end{bmatrix}, \end{aligned}$$

where $X \in \mathbb{R}^{22}$ and $U \in \mathbb{R}^4$. In the following, the model equations are lumped into the function:

$$\dot{X} = f(X,U).$$

III. An NMPC formulation for Aircraft Control

In this Section, an NMPC formulation for aircraft control is described in detail. The handling of the flight envelope is treated in Subection III-B, the problem of actuator failure is treated in Subsection III-C, and obstacle avoidance in Subsection III-D. The NMPC formulation is given is Subsection III-E. Next, a computationally inexpensive way of computing a reference for the attitude is proposed.

A. Attitude reference

In this paper, a piecewise differentiable reference trajectory for the position $\gamma(t)$ is provided to the aircraft controller. A reference for the aircraft velocity v is readily given by $\dot{\gamma}(t)$. However, providing a reference for the attitude-related states improves significantly the numerical behavior of the resulting NMPC scheme. A computationally inexpensive way to compute a reasonable reference for the aircraft attitude is to choose the aircraft longitudinal axis e_1 collinear with the reference velocity, and the vertical aircraft axis e_3 collinear with the acceleration of the reference trajectory, i.e. $\ddot{\gamma}+g\mathbf{1}_3$. The reference for the aircraft attitude can be therefore computed using:

$$\begin{gathered} a=\ddot{\gamma}+g\mathbf{1}_3, \quad L=a-\langle a,e_1\rangle e_1, \\ e_1^{\text{ref}}=\|\dot{\gamma}\|^{-1}\dot{\gamma}, \quad e_3^{\text{ref}}=\frac{L}{\max(\|L\|,g)}, \quad e_2^{\text{ref}}=e_3^{\text{ref}}\times e_1^{\text{ref}} \end{gathered} \tag{2}$$

The proposed choice of e_3^{ref} is aimed at dealing with zero-G situations, i.e. when L drops to zero. In such a case, the vertical axis is no longer defined, and the references e_3^{ref}, e_2^{ref} drop to zero until a vertical axis is recovered.

B. Flight envelope

The control is based on repeatedly solving an optimal control problem (OCP) providing input sequences that best track a given reference trajectory, while respecting the aircraft flight envelope and actuators limitation. In this paper, it is proposed to formulate the aircraft flight envelope using a set of inequality constraints. The following constraints for the flight-envelope are proposed:

- Stall: $C_{\text{L}}^{\min} \leq C_{\text{L}} \leq C_{\text{L}}^{\text{stall}}$
- Maximum relative velocity: $V \leq V_{\text{NE}}$
- Maximum lift force: $|e_3^T F| \leq F_3^{\max}$
- Maximum roll torque: $|T_{\text{R}}| \leq T_{\text{R}}^{\max}$

Because flight envelope constraints are mixed or pure state constraints, their feasibility under perturbations cannot be guaranteed. To tackle that issue, a slack reformulation has to be considered, together with a back-off from the original constraint. Writing down the flight-envelope constraints as:

$$h(X,U) \leq h^{\max}, \tag{3}$$

where

$$h(X,U)=\begin{bmatrix} C_{\text{L}} \\ -C_{\text{L}} \\ V \\ e_3^T F \\ -e_3^T F \\ T_{\text{R}} \\ -T_{\text{R}} \end{bmatrix}, \quad h^{\max}=\begin{bmatrix} C_{\text{L}}^{\max} \\ -C_{\text{L}}^{\min} \\ V_{\text{NE}} \\ F_3^{\max} \\ F_3^{\max} \\ T_{\text{R}}^{\max} \\ T_{\text{R}}^{\max} \end{bmatrix},$$

a scaled, relaxed formulation of (3) reads:

$$\frac{h_i(X,U)}{(1-\varepsilon_i)\,h_i^{\max}} - S_i \leq 1, \quad 0 \leq S_i, \;\; i=1,...,7. \tag{4}$$

where $S_i \in \mathbb{R}$ is a positive slack variable, and ε_i is a constant relative back-off parameter for the i^{th} constraint. Slack variables S_i become positive as soon as $h_i > (1-\varepsilon_i)\,h_i^{\max}$.

C. Actuator failure

For the sake of brevity, only failures of the control surfaces are considered in this paper, though a larger set of failures can be easily considered.

Control surface failure is often associated to a loss of hydraulic pressure in the actuator power system, resulting in a quick loss of mobility of the corresponding control surface. This type of actuator failure can be modeled as a fast reduction of the corresponding bounds $-\dot{u}_{\max}^i \leq \dot{u}_i \leq \dot{u}_{\max}^i$ down to a small value, yielding a very limited mobility of the control surface. It is proposed here to use a constant rate for the loss of mobility, i.e. if control surface i fails, then:

$$\dot{u}_{\max}^i = \text{sat}_{\varepsilon_{\text{fail}}}\left(1+\frac{T_{\text{fail}}-t}{\Delta t_{\text{fail}}}\right),$$

where T_{fail} is the time of actuator failure, Δt_{fail} is the time to total loss, $\varepsilon_{\text{fail}}$ is the residual mobility, and sat is the saturation function trimming the function argument to the set $[\varepsilon_{\text{fail}}, 1]$.

In the case of a control surface failure, the control action must be concentrated on recovering a safe, level-flight attitude. A level-flight reference attitude is therefore provided to the controller, with a free heading, i.e. the deviations of $e_{1,2,3}$ from the references:

$$e_3^{\text{ref}} = \begin{bmatrix} 0 & 0 & 1 \end{bmatrix}, \quad \left(e_1^{\text{ref}}\right)_z = 0, \quad \left(e_2^{\text{ref}}\right)_z = 0$$

are penalized, while the weight corresponding to the states $(e_{1,2})_{x,y}$, x, y, $\dot{x}$, $\dot{y}$ are set to zero. The vertical position and velocity, z and $\dot{z}$ are penalized.

D. Obstacle avoidance

In this paper, obstacles are defined by balls $\mathcal{B}^k\left(p_{\text{O}}^k, R_{\text{O}}^k\right)$ at positions p_{O}^k and of radius R_{O}^k. More elaborate shapes such as cylinders, ellipsoids or polyhedra can be equally easily considered. Avoidance of ball-shaped obstacles can be performed by satisfying the non-convex set of quadratic inequality constraints:

$$\left\|p-p_{\text{O}}^k\right\|^2 \geq \left(R_{\text{O}}^k\right)^2 \tag{5}$$

A scaled, relaxed formulation of (5) reads:

$$\begin{gathered} \left(1+\varepsilon_{\text{O}}^k\right)^{-2}\left(R_{\text{O}}^k\right)^{-2}\left\|p-p_{\text{O}}^k\right\|^2 + S_{\text{O}}^k \geq 1 \\ 0 \leq S_{\text{O}}^k, \quad k=1,...,N_{\text{O}}, \end{gathered} \tag{6}$$

where $S_{\text{O}}^k \in \mathbb{R}$ is a positive slack variable, and ε_{O}^k a relative back-off. Slack variable S_{O}^k becomes positive as soon as $\left\|p-p_{\text{O}}^k\right\|^2 < \left(\left(1+\varepsilon_{\text{O}}^k\right)R_{\text{O}}^k\right)^2$.

In the case of obstacle avoidance, large excursion from the position references can be required, hence the weights

on the position x,y,z are set to zero until the obstacles are cleared, and then gradually restored to their normal values.

E. NMPC problem formulation

The NMPC scheme is based on repeatedly solving the optimal control problem (OCP):

$$\begin{aligned} P = \min_{X,U,S} \quad & W^T S + \int_t^{t+T_h} \left(\|X - \bar{X}\|_Q^2 + Q_\beta \beta^2 + \|U\|_R^2 \right) dt \\ s.t. \quad & \dot{X} = f(X,U), \quad X(t) = \hat{X}(t) \\ & (4) \ \& \ (6), \quad |u_j| \leq u_{\max}^j, \quad j = 1,2,3 \\ & U_{\min} \leq U \leq U_{\max}, \quad 0 \leq u_4 \leq 1, \end{aligned} \tag{7}$$

where Q and R are positive semi-definite and positive definite matrices respectively, vector $S = [S_h \ S_O]^T \in \mathbb{R}^{7+N_O}$ is a vector of slack variables, $\hat{X}(t)$ is the aircraft state vector at time t, and $\bar{X}$ is a time-varying state reference.

IV. Real-time solution approach

Repeatedly computing reliable solutions to OCP (7) in real time is a challenging task. In this section, a solution approach to achieve a real-time implementation of the NMPC controller is presented.

A. Multiple-shooting & real-time iteration

Because the model dynamics $\dot{X} = f(X,U)$ are unstable and because a prediction horizon T_H of several seconds needs to be considered, the optimization shall be performed using simultaneous approaches [1]. A direct multiple-shooting approach was chosen [2], where the model dynamics are discretized on a uniform time grid $t_0, ..., t_N$ by numerical integration over the time intervals $[t_k, t_{k+1}]$. The control input U is discretized as piecewise constant $U_0, ..., U_{N-1}$ over the time intervals. The inequality constraints are discretized on the same time grid. The discretized OCP is a medium-scale structured Non-Linear Program (NLP).

After each iteration, the initial guess for problem (7) is updated by discarding the first element, shifting the state and input vectors X, U, and adding a new element at the end of the prediction horizon. The control inputs are updated by duplicating the last element, and the states are updated using a forward integration on the last time interval.

If an initial value embedding is introduced in the subsequent problems [4], the first Newton step resulting from such an initial guess provides already a good approximation of the exact solution to problem (7), hence a real-time iteration (RTI) approach is used, where only one step per control interval needs to be performed. Moreover, most computations required to perform the first Newton step can be performed before the new initial conditions $X(t)$ are known. As a result, the re-calculation of the control inputs can be prepared before the new state estimation is known, and finished in a very short time once it becomes available, hence reducing significantly the delay between state estimation and control in the NMPC scheme [3].

TABLE I
Model parameters

Parameter	Value	Unit
m_A, A	$6 \cdot 10^3$, 100	(kg), (m^2)
diag(I)	$[4.4 \cdot 10^3 \ \ 2.1 \cdot 10^3 \ \ 6.2 \cdot 10^3]$	($kg \cdot m^2$)
ρ	1.23	($kg \cdot m^{-3}$)
τ_h, L^e, L_t	1.5, 0.1, $-15 \cdot \mathbf{1}_x$	(s), (m), (m)
α_0^t, C_L^α, ε_O	-10, 3.82, 0.05	(deg), (-), (-)
C_D^0, C_D^α, C_D^β	10^{-2}, 0.25, 0.1	-
C_R^u, C_R^l, C_R^3	0.1, -4, 1	-
C_P^u, C_P^l, C_P^α	0.1, 7.5, 1	-
C_Y^u, C_Y^l, C_Y^T	0.1, 0.1, 7.5	-
ε_{fail}, Δt_{fail}	0.5, 5	(deg/s), (s)
$\dot{u}_4^{max}$, T_{max}	0.5, 10	(1/s), (kN)
u_{max}, $\dot{u}_{max}$	30, 10	(deg), (deg/s)
C_L^{max}, $\varepsilon_{C_L^{max}}$	1.5, 0.2	(-), (-)
C_L^{min}, $\varepsilon_{C_L^{min}}$	-0.2, 0.2	(-), (-)
F_3^{max}, $\varepsilon_{F_3^{max}}$	$1.8 \cdot 10^5$, 0.17	(N), (-)
T_R^{max}, $\varepsilon_{T_R^{max}}$	$8.4 \cdot 10^4$, 0.17	(Nm), (-)
V_{NE}, $\varepsilon_{V_{NE}}$	63, 0.05	(m/s)

B. Software approach

In this paper, numerical solutions to problem (7) were computed using the software ACADO Toolkit [7], based on direct multiple-shooting, RTI and a Sequential Quadratic Programing (SQP) method. The underlying Quadratic Programs (QP) are condensed and solved using an online active set strategy implemented in the software qpOASES [5].

SQP methods are known to be highly competitive in term of computational speed for small to medium-scale problems. However, the performance of alternative approaches such as interior-point techniques should be compared to the proposed approach. This comparison is beyond the scope of this paper.

V. Simulation results

The trajectory $\gamma(t) \in C^0$ is provided to the controller for the interval $[t, t+T_H]$. A prediction horizon $T_H = 10\ s$ was chosen, with $N = 20$ control intervals. The weighting matrices are chosen as:

$$\begin{aligned} Q &= \mathrm{diag}\left([0.1 \ \ 0.1 \ \ 1 \ \ 1 \ \ 1 \ \ 1 \ \ 10 \cdot \mathbf{1}_{1\times 9} \ \ 1 \ \ 1 \ \ 1]\right), \\ R &= \mathrm{diag}\left(\begin{bmatrix} 0.1 & 0.1 & 0.1 & 1 \end{bmatrix}\right). \end{aligned}$$

The position and velocity reference are obtained directly from γ and $\dot{\gamma}$. The attitude reference is computed according to (2). The references for all remaining states are set to zero. The model and control parameters used for the following simulations are listed in Table I.

The matrices Q and R have a strong impact on the control performance. Moreover, the final time T_f must be chosen long enough to achieve stability in the region of interest, but short enough so that changes of reference trajectories can be accomodated at a relatively short notice. The choice of Q, R and T_f was straightforward in the proposed example, but should be more systematically explored in the future.

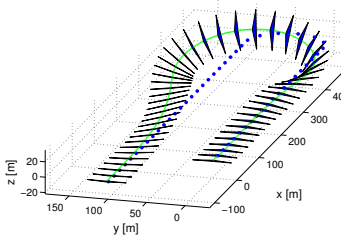


Fig. 2. Fast turn, 3D trajectory. The dotted curve is the reference trajectory γ. The aircraft trajectory is the solid line.

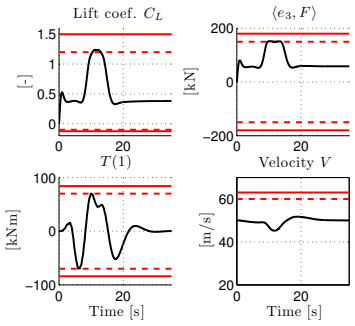


Fig. 3. Fast turn, flight envelope. The dashed lines are the constraints with back-off, the solid lines are the physical constraints.

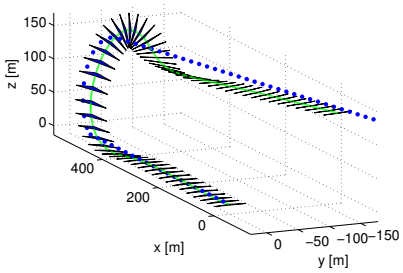


Fig. 4. Flip, 3D trajectory. The dotted curve is the reference trajectory γ. The aircraft trajectory is the solid line.

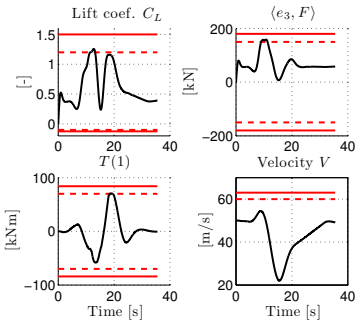


Fig. 5. Flip, flight envelope. The dashed lines are the constraints with back-off, the solid lines are the physical constraints.

A. Real-time implementation

The choice of discretization requires that solutions to the NMPC problem (7) are computed faster than $T_H/N = 500$ ms. To achieve this goal, the softwares described in Subsection IV-B are implemented in code generation, where the compiled code is automatically tailored to the problem considered, and contains only the absolutely essential algorithmic components. Based on a symbolic representation of the optimal control problem to be solved online, problem-specific structure such as dimensions, sparsity patterns etc. is exploited during the code generation process to avoid irrelevant and redundant computations (see [8], [6]). The generated code was executed on a 2.4 GHz/64 bits CPU with a cache size of 3072 kB. The execution time required to compute solutions to the NMPC problem (7) was of the order of 30 ms, hence 15 times faster than necessary for the proposed example. Future work will exploit that discrepancy to explore systematically the control performance in term of increased controller sampling frequencies T_H/N.

B. Fault-free control

Two scenarios are considered to illustrate the fault-free behavior of the proposed control scheme: a) a tight U-turn and b) a flip manoeuvre. For both maneuvers, an infeasible trajectory $\gamma(t) \in C^0$ is provided. The corresponding aircraft 3D trajectories and attitude can be observed in Figures 2 and 4. The resulting flight envelope constraints can be seen in Figures 3 and 5. In both cases, the NMPC uses the full flight envelope in order to best track the reference trajectory.

C. Actuator failure

To illustrate the behavior of the NMPC as a fault-tolerant controller, a failure of the aileron actuator is simulated. Figure 6 displays the resulting 3D trajectory and aircraft attitude and the flight envelope can be seen in Figure 7. The loss of aileron mobility can be seen in Figure 8, upper graph.

D. Obstacle avoidance

A situation of emergency obstacle avoidance is simulated. The obstacles were introduced in the NMPC constraints about 2 s before impact, resulting in an extreme manoeuvre. The aircraft 3D trajectory and attitude can be seen in Figure 9. Respecting the constraint associated to the first obstacle is not feasible, hence the trajectory enters slightly into the first sphere (see Figure 9). The NMPC uses the full flight

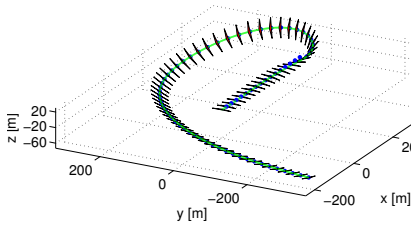


Fig. 6. Aileron failure in a sharp turn, 3D trajectory. The aircraft trajectory is the solid line. The aircraft attitude is represented by the triangles.

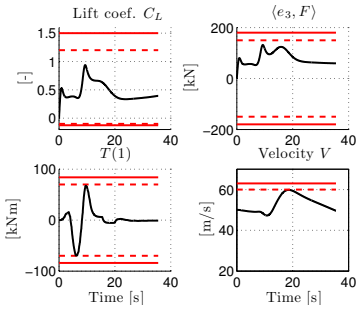


Fig. 7. Ailerons failure in a turn, flight envelope

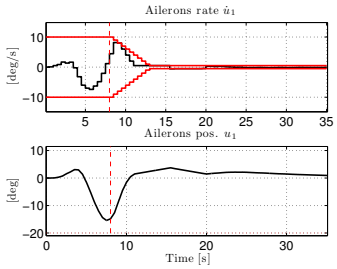


Fig. 8. Ailerons failure in a turn, ailerons rate and position

envelope in order to perform the manoeuvre (see Figure 10).

VI. Conclusion & Further Developments

This paper has proposed an aircraft model and NMPC formulation dedicated to aircraft control through extreme maneuvers. The control scheme can handle infeasible reference trajectories, deal with actuator failure and obstacle avoidance. A solution approach to solve the resulting NMPC in real-time is presented, the time required to update the NMPC control inputs is 30 ms and can therefore be safely used for a real-time implementation. The proposed control approach is validated in simulations, for two examples of extreme maneuvers, an example of aileron failure, and an example of obstacle avoidance.

Future work will expend the proposed scheme to actuator and sensor fault identification, explore its robustness toward model errors, and assess its reliability with respect to the non-convexity of the underlying optimization problem.

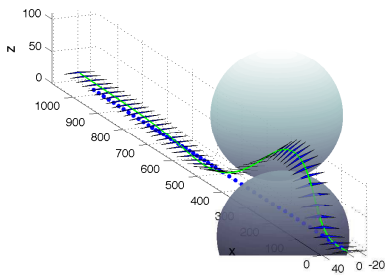


Fig. 9. Obstacle avoidance, 3D trajectory.

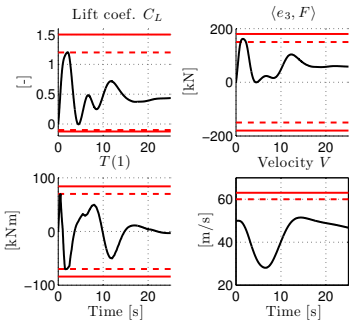


Fig. 10. Obstacle avoidance, flight envelope

VII. Acknowledgments

This research was supported by Research Council KUL: PFV/10/002 Optimization in Engineering Center OPTEC, GOA/10/09 MaNet and GOA/10/11 Global real- time optimal control of autonomous robots and mechatronic systems. Flemish Government: IOF/KP/SCORES4CHEM, FWO: PhD/postdoc grants and projects: G.0320.08 (convex MPC), G.0377.09 (Mechatronics MPC); IWT: PhD Grants, projects: SBO LeCoPro; Belgian Federal Science Policy Office: IUAP P7 (DYSCO, Dynamical systems, control and optimization, 2012-2017); EU: FP7-EMBOCON (ICT-248940), FP7-SADCO (MC ITN-264735), ERC ST HIGHWIND (259 166), Eurostars SMART, ACCM.

References

[1] L.T. Biegler. An overview of simultaneous strategies for dynamic optimization. *Chemical Engineering and Processing*, 46:1043–1053, 2007.

[2] H.G. Bock and K.J. Plitt. A multiple shooting algorithm for direct solution of optimal control problems. In *Proceedings 9th IFAC World Congress Budapest*, pages 243–247. Pergamon Press, 1984.

[3] M. Diehl, H.G. Bock, J.P. Schlöder, R. Findeisen, Z. Nagy, and F. Allgöwer. Real-time optimization and Nonlinear Model Predictive Control of Processes governed by differential-algebraic equations. *J. Proc. Contr.*, 12(4):577–585, 2002.

[4] M. Diehl, R. Findeisen, S. Schwarzkopf, I. Uslu, F. Allgöwer, H.G. Bock, E.D. Gilles, and J.P. Schlöder. An Efficient Algorithm for Nonlinear Model Predictive Control of Large-Scale Systems. Part I: Description of the Method. *Automatisierungstechnik*, 50(12):557–567, 2002.

[5] H.J. Ferreau. An Online Active Set Strategy for Fast Solution of Parametric Quadratic Programs with Applications to Predictive Engine Control. Master's thesis, University of Heidelberg, 2006.

[6] H.J. Ferreau. *Model Predictive Control Algorithms for Applications with Millisecond Timescales*. PhD thesis, K.U. Leuven, 2011.

[7] B. Houska, H.J. Ferreau, and M. Diehl. ACADO Toolkit – An Open Source Framework for Automatic Control and Dynamic Optimization. *Optimal Control Applications and Methods*, 32(3):298–312, 2011.

[8] B. Houska, H.J. Ferreau, and M. Diehl. An Auto-Generated Real-Time Iteration Algorithm for Nonlinear MPC in the Microsecond Range. *Automatica*, 47(10):2279–2285, 2011.

[9] M.M Kale and Chipperfield A.J. Reconfigurable Flight Control Strategies Using Model Predictive Control. In *International Symposium on Intelligent Control*, 2002.

[10] T. Keviczky and G. Balas. Receding Horizon Control of an F-16 Aircraft: A Comparative Study. *Control Engineering Practice*, 14:1023–1033, 2006.

[11] M.L. Loyd. Crosswind Kite Power. *Journal of Energy*, 4(3):106–111, July 1980.

[12] J.M. Maciejowski and C.N. Jones. MPC Fault-tolerant Flight Control Case Study: Flight 1862. In *IFAC Safeprocess Conference, Washington DC*, 2003.

[13] J.P. Ruiz. *Reconfigurable Autopilot Design for a High Performance Aircraft Using Model Predictive Control*. PhD thesis, Massachusetts Institute of Technology, 2004.